

극 천해 다중경로 페이딩 채널 특성과 전방오류 정정 코드의 성능

배민자 · 설단단 · 박지현 · 윤종락*

Multipath Fading Channel Characterization and Performances of Forward Error Correction Codes in Very Shallow Water

Minja Bae · Xue Dandan · Jihyun Park · Jong Rak Yoon *

Dept. of Information and Communications Engineering, Pukyong National University, Busan 608-737, Korea

요 약

극 천해 음향 통신 채널에서 수중 음향 통신 신호는 시변 다중 경로에 의해 주파수 선택적인 페이딩 신호로 관측된다. 이러한 특성으로 시간 및 주파수에 따라 심벌간의 간섭이 변화하고 수중 통신 시스템의 성능이 저하된다. 오류 정정 코드의 성능이 어떻게 극 천해 다중경로 페이딩의 통계적 특성과 관계되는지에 대한 연구는 전무하다. 본 연구에서는 다중경로 채널의 특성을 해석하고 2가지 전방 오류 정정 코드를 적용하여 극 천해 다중 경로 채널에서 이들의 성능을 비교하였다. 컨벌루션 코드와 Reed-Solomon 코드를 적용한 해상 실험 결과는 Reed-Solomon 코드가 주파수 선택적인 페이딩 채널에서 컨벌루션 코드 보다 우수함을 보였다.

ABSTRACT

In very shallow water acoustic communication channel, underwater acoustic (UWA) communication signal is observed as frequency selective fading signal due to time-varying multipath. This induces a time and frequency dependent inter-symbol-interference (ISI) and degrades the UWA system performance. There is no study about how the performances of the error correction codes are related to a multipath fading statistics in very shallow water. In this study, the characteristics of very shallow water multipath fading channel is analyzed and the performances of two different forward error correction (FEC) codes are compared. The convolution code (CC) and Reed-Solomon (RS) code are adopted. Sea experimental results show that RS code is better choice than CC in frequency selective channel with fading.

키워드 : 다중경로 채널, 페이딩, 수중 음향 통신, 전방 오류 정정코드, 주파수 선택성, 시간 일관성.

Key word : Multipath channel, Fading, Underwater acoustic communication, Forward error correction code, Frequency selectivity, Temporal coherence

Received 13 July 2015, Revised 04 August 2015, Accepted 19 August 2015

* Corresponding Author Jong Rak Yoon (E-mail:jryoon@pknu.ac.kr, Tel:+82-51-629-6233)

Dept. of Information and Communications Engineering, Pukyong National University, Busan 608-737, Korea

Open Access <http://dx.doi.org/10.6109/jkiice.2015.19.10.2247>

print ISSN: 2234-4772 online ISSN: 2288-4165

©This is an Open Access article distributed under the terms of the Creative Commons Attribution Non-Commercial License(<http://creativecommons.org/licenses/by-nc/3.0/>) which permits unrestricted non-commercial use, distribution, and reproduction in any medium, provided the original work is properly cited.
Copyright © The Korea Institute of Information and Communication Engineering.

I. Introduction

In very shallow water, underwater acoustic (UWA) communication channel is influenced by environmental parameters such as multipath, scattering and background noise. Furthermore, the channel is time-varying and a degree of time varying depends on source and receiver motion, sea surface fluctuation, medium property fluctuation, and so on[1,2]. Therefore a received signal shows a delay spread and a Doppler spread. A long delay spread limits available coherent channel bandwidth B_c and increase frequency selectivity. A wide Doppler spread or short coherent time T_c limits a transmitted signaling interval. A delay spread and a Doppler spread are also interpreted as a frequency domain fading and a time domain fading, respectively.

To cope with adverse effects of both spreads on underwater acoustic communication system, frequency and time diversity techniques are adopted in fading multipath channels. These may be viewed as the transmission of the same information either at different frequencies or in different time slots. The separation of the diversity transmissions in frequency by B_c or in time by T_c is basically a form of redundant code in an attempt to break up the error burst and thus to obtain independent errors.

The performance of BFSK has been studied to quantify the bit-error-rate(BER) as a function of a delay spread and a transmission rate for a fixed carrier frequency[3,4].

The frequency diversity technique FH/FSK (frequency hopping frequency shift keying) for high speed data transmission has adopted to reduce a carrier frequency dependent BER for a given delay spread[5]. The simulation results shows that the proposed FH/FSK can be applied as underwater acoustic communication system without a channel coding.

The time diversity technique such as a convolution code(CC) and Reed-Solomon(RS) code has been applied in underwater acoustic communication systems[6-8]. The

error correcting capability of CC is found to be better than RS in frequency non-selective multipath channel but vice versa in frequency selective channel. However, these studies do not consider time variant multipath fading statistics which depends on frequency dependent multipath interference.

In this study, the characteristics of very shallow water multipath fading channel is analyzed and the performances of two different forward error correction (FEC) codes are compared based on multipath channel characteristics. The convolution code (CC) and Reed-Solomon (RS) code are adopted.

II. Very Shallow Water Multipath Fading Channel

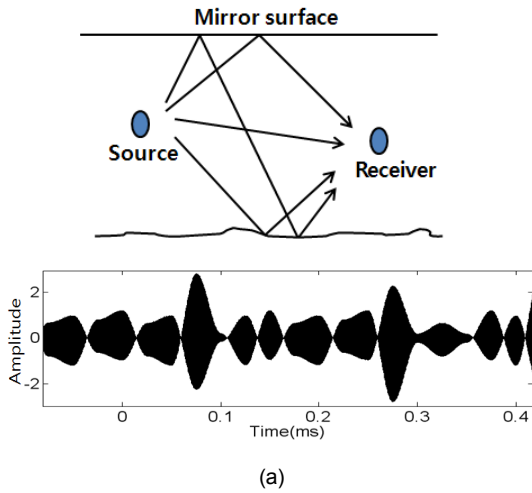
Fig. 1(a) and 1(b) show typical multipath channels and received signals waveform. Both figures show a signal fading principle due to interference of multipath. In the channel of Fig. 1(a) which depicts a time invariant multipath channel, the received signal is measured as a time variant signal due to a long delay spread or a narrow channel bandwidth with a high speed transmission rate or a wide signal bandwidth. In the channel of Fig. 1(b) which depicts a time variant multipath channel, the received sinusoid signal is also measured as a time variant signal envelope due to a Doppler spread.

For the time invariant of multipath channel such as Fig.1(a), the time invariant channel impulse response $h(t)$ given as

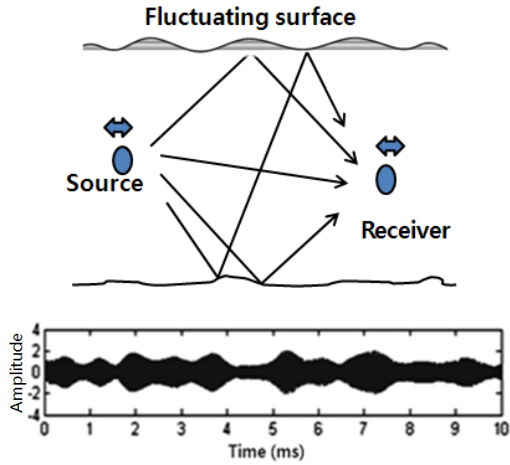
$$h(t) = \sum_{n=0}^N \alpha_n e^{-j2\pi f_c \tau_n} \delta(t - \tau_n). \quad (1)$$

Here, α_n and τ_n are the n th path signal amplitude and delay time. If the coherent channel bandwidth B_c which is given as a function of the effective delay spread τ_{eff} , is less than the signal bandwidth B_s , a

distortion occurs within the signal bandwidth and the signal waveform exhibits a fading as in Fig. 1(a). Therefore each information bearing base band signal has a different signal-to-noise ratio (SNR). The channel in this case is defined as a frequency selective.



(a)



(b)

그림 1. (a) 주파수 선택적인 다중경로 채널 및 이진 주파수 편이변조 수신신호 (b) 해면 산란과 송수신기 운동에 의한 정현신호의 수신신호

Fig. 1 (a) Frequency selective multipath channel and received signal waveform of binary phase shift keying signal (b) Received signal waveform of sinusoid due to surface scattering and source-receiver movement

In the case of Fig. 1(b), the time variant impulse response $h(\tau, t)$ of band pass communication system is given as[9]

$$h(\tau, t) = \sum_n \alpha_n(t) e^{-2\pi f_c \tau_n(t)} \delta(\tau - \tau_n(t)) + \beta(\tau, t) e^{-2\pi f_c \tau} \quad (2)$$

The first and second terms show discrete and continuous multipath components, respectively. The $\alpha_n(t)$ is then the multipath signal time variant amplitude which depends on time variant boundary reflection coefficient, propagation path loss, and frequency dependent absorption loss, and $\tau_n(t)$ is the n th multipath time variant delay time. $\beta(\tau, t)$ is a continuous multipath time variant amplitude. Therefore received signal amplitude of band pass system will be faded and the statistics of fading signal envelope $|h(\tau, t)|$ such as Rayleigh or Rice distribution is related to multipath structure.

The autocorrelation function of $h(\tau, t)$ is defined as

$$R_h(\tau_1, \tau_2; \Delta t) = \frac{1}{2} E[h^*(\tau_1; t) h(\tau_2; t + \Delta t)], \quad (3)$$

where Δt is an observation time difference between two different time instant $h(\tau, t)$. If the observation time difference Δt is set to be 0, then $R_h(\tau_1, \tau_2; 0)$ becomes a multipath intensity profile (MIP). Fourier transform of the autocorrelation function $R_h(\tau_1, \tau_2; 0)$ gives a channel coherence bandwidth B_c .

In time-varying underwater channel, the signal temporal coherence is used to describe the rate of the signal fluctuation depending on Doppler spread. The higher the signal fluctuation, the faster the temporal coherence decreases with time. Temporal coherence is defined by the correlation of the signals separated by a delay time, normalized by the power of the signal, as given by

$$\rho(t, \tau) = \left\langle \frac{[p^*(t) \otimes p(t + \tau)]_{\max}}{\sqrt{[p^*(t) \otimes p(t)]_{\max} [p^*(t + \tau) \otimes p(t + \tau)]_{\max}}} \right\rangle, \quad (4)$$

where $[p^*(t) \otimes p(t)]_{\max}$ means the maximum value of the cross-correlation of the two time series or the convolution of the time-reversed signals (denoted by *) with the other signal[10]. A slowly or fast fading channel is defined by large or small coherence time.

III. Forward Error Correction Codes

In communication channels, errors can occur independently at random, burst, or in a mixed manner. The forward error correction (FEC) codes scheme has been applied to combat these errors. Without an interleaving, a convolution code(CC) has been known to be effective for a random error correcting but Reed-Solomon to be more effective in correcting burst errors.

The CC is generally specified by three parameters (n , k , m), where n is the number of encoder output bits corresponding to the k information bits and k is the number of bits shifted into the encoder at one time. m is the constraint length or the number of input data bits that the current output is dependent upon. As shown in Fig. 1, the number of output bits ($n=2$) is twice that of input bits ($k=1$) and the constraint length is 3 corresponding to two shift registers plus one input.

The RS code (n, k, t) is a non-binary cyclic code and known to be capable of correcting errors which appear in burst. n, k , and t are the block code length, message length, and error correcting symbols, respectively. $n-k$ and $t=(n-k)/2$ are the measure of redundancy in the block and the number of correctable symbols, respectively.

In this study, QPSK/CC (2,1,3) and QPSK/RS (7,3,2), which give similar redundancies of 2 and 2.2, are applied to compare error correction performance.

IV. Experiment

Fig.2 shows schematic diagram of sea experimental configuration in very shallow multipath channel environment. The experiments were conducted in the bay of the Geo-je Island. The experimental parameters are shown in Table 1. The depth is about 15.7 m, the effective height of sea surface is about 0.1 to 0.3 m and bottom sediment is mud. The distance between the source (ITC 1001) and receiver (B&K 8106) are set to be about 100 and 400 m for a range difference effect. Transmitter and receiver are positioned asymmetrically in a middle layer to get a large time delay difference between multi-paths as possible. The depth of source and receiver are 10 and 7 m, respectively.

Fig. 3(a) is sound velocity profile (SVP) analyzed by the conductivity, temperature, and depth. In Fig. 3(b), the numerical value of each eigenray means grazing angle with respect to sea surface plane and only the first five arrivals which could show high signal amplitude are shown.

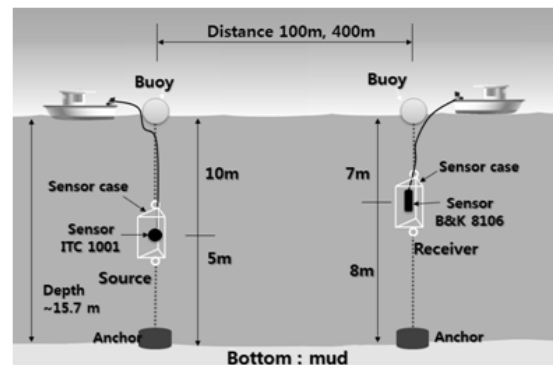
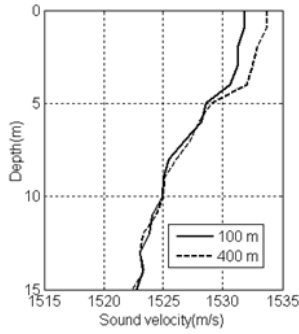


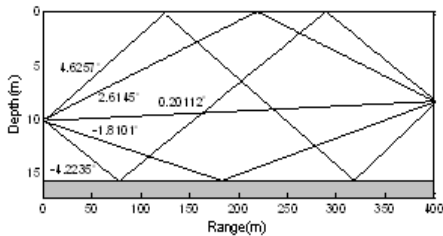
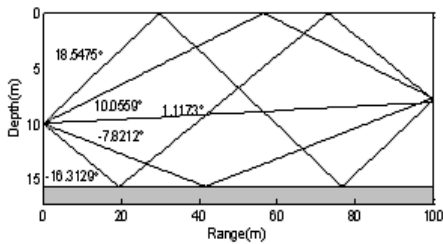
그림 2. 실험 구성도
 Fig. 2 Schematic diagram of sea experimental configuration

Fig. 4 shows a transmission frame structure for 1 second, which is composed of a synchronization signal and information signal. The pseudo noise (PN) signal of modulated by 16 kHz (128 bit) is used for frame synchronization. The bandwidth of PN signal is 13 to 19

kHz. Before data transmission in each source to receiver range, 30s of PN signal is transmitted to measure the channel impulse response, temporal coherence and fading statistics of channel.



(a)



(b)

그림 3. 송수신기 거리 100m와 400m의 음속구조 및 모의 음선 궤적. (a) 음속 구조 (b) 음선궤적

Fig. 3 (a) Sound speed profiles, and (b) simulated eigenray traces for two different source-receiver ranges (100 and 400 m)

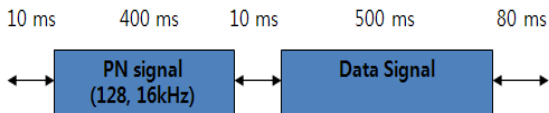


그림 4. 전송 프레임 구조.

Fig. 4 Transmission frame structure.

표 1. 실험 파라미터

Table. 1 The Sea experimental parameters

Modulation	QPSK
Carrier frequency (kHz)	16
FEC codes	convolutional code (2,1) Reed-Solomon code (7,3,2)
Symbol rate (sps)	100, 200, 400
Tx-Rx Range (m)	100, 400
Tx-Rx depth (m)	10, 7
Water depth (m)	~ 15.7
Wave height (m)	0.1~0.3
Bottom property	mud
Transmission bit	10,000

V. Results and Discussions

Fig. 5(a) and 5(b) show multipath intensity profiles for 100 and 400 m, respectively. By using the relation between multipath intensity profile or delay spread and channel coherent bandwidth, -3 dB coherent bandwidths of 100, and 400 m are found to be 60 and 200 Hz, respectively.

Fig. 6(a) and 6(b) shows power spectrum of received PN signal. There are dips and maxima which show destructive and constructive interference frequencies in PN signal bandwidth.

Fig. 7 shows fading statistics of 100 and 400 m at carrier frequency of 16 kHz with 100 Hz bandwidth. The fading statistics of 100 and 400 m follow Rayleigh and Rice distribution, respectively. By considering the dips in Fig. 6(a) for 100 m range, since a destructive interference appears at 16 kHz and so there is not any dominant component in this frequency band, the first term in eqn. (2) is ignored and the channel statistics will be Rayleigh distribution. However, in Fig. 6(b) for 400 m range, since 16 kHz locates in a constructive interference range and so the first term in eqn. (2) can not be ignored, the channel statistics will be Rice distribution.

Fig. 8 shows temporal coherence distributions for 100 and 400m ranges using eqn. (4).

The temporal coherence of 100 m drops to 0.88 in about 0.5 s but the temporal coherence of 400 m shows about 0.96. It is clear that Doppler spread of both ranges are less than 1 Hz by the formula given in previous study.

Temporal coherence variation with time seems to mimic well the surface fluctuation. The variation magnitude of 100 m range is larger than that of 400 m since relative motion of sea surface at 100 m range is greater than that of 400 m range.

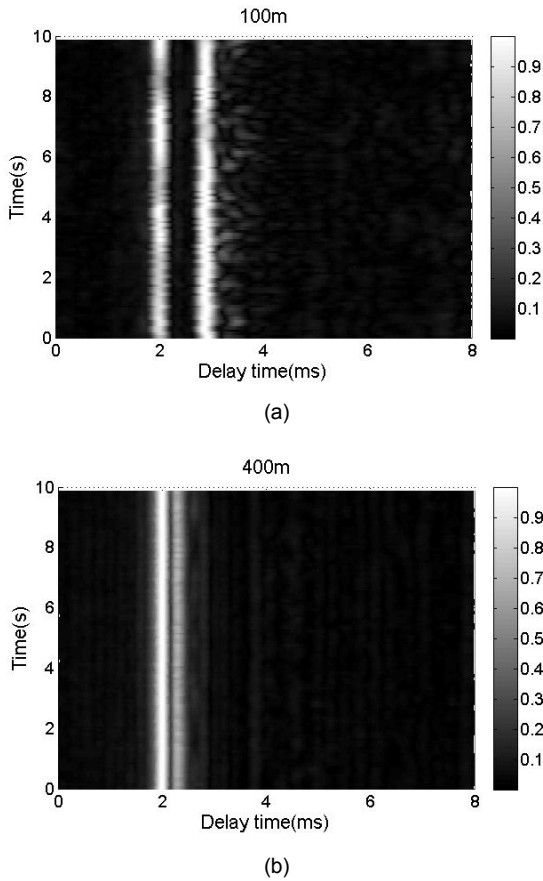


그림 5. 송수신기 거리 (a) 100m와 (b) 400m의 다중경로 세기 응답
 Fig. 5 Measured multipath profiles as a function of the delay time and geotime (a) 100m (b) 400m

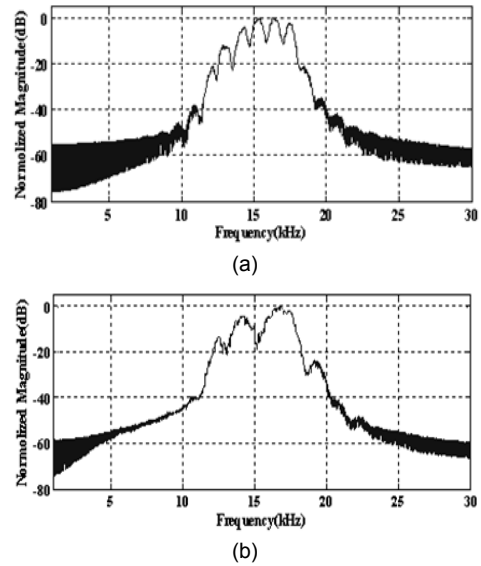


그림 6. 송수신기 거리 (a) 100m와 (b) 400m의 PN 수신 신호 스펙트럼

Fig. 6 Normalized receiving signal spectra of PN signals (a) 100m (b) 400m

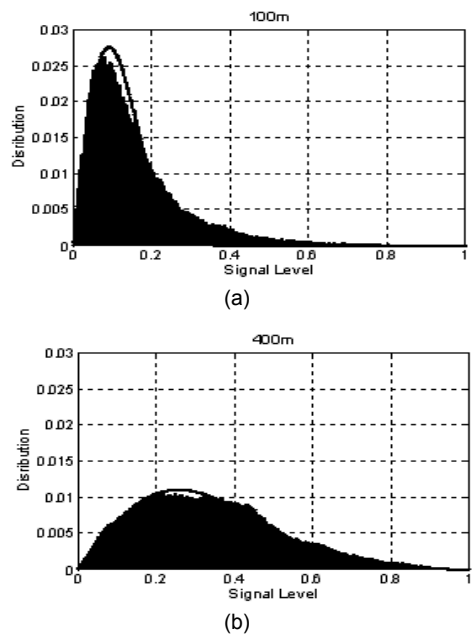


그림 7. 송수신기 거리 100m와 400m의 PN 수신신호의 16kHz, 100Hz 대역의 확률 밀도 함수 (a) 100m (b) 400m

Fig. 7 Probability density of received PN signal amplitude envelopes at 16 kHz with 100 Hz bandwidth (a) 100m (b) 400m

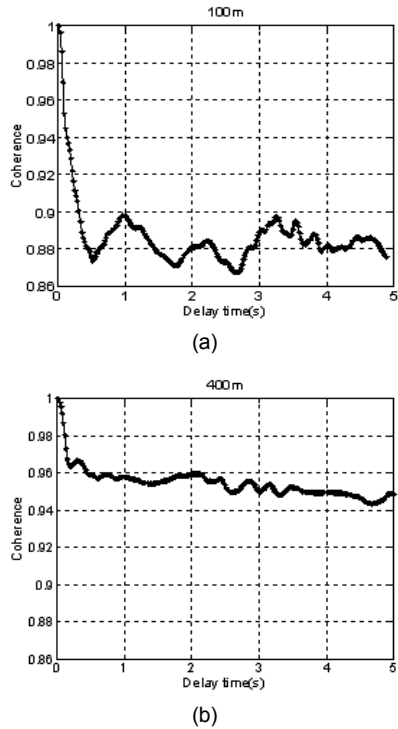


그림 8. 시간 일관성 (a) 100m (b) 400m
 Fig. 8 Temporal coherences (a) 100m (b) 400m

Table 2 shows the results for performances of RS and CC at 100 m range and three different symbol rates (100, 200 and 400 symbol per second (sps)). Signal bandwidth of each symbol rate is larger than channel coherent bandwidth of 60 Hz. Probability density is Rayleigh distribution as shown in Fig. 7(a). All the BERs of RS is less than that of CC.

Table 3 shows results for performances of RS and CC at 400 m range. The channel coherent bandwidth and probability density are 200 Hz and Rice distribution, respectively. Only the signal bandwidth of 100 sps is less than channel coherent bandwidth of 200 Hz. In this case the BER of CC is less than that of RS. This result confirms that authors' previous water tank experiment result which shows that error correcting capability of RS is worse than CC in frequency non-selective channel but RS is better than CC in frequency selective channel[8].

표 2. 송수신기 거리 100m에서 컨벌루션과 Reed-Solomon 코드의 비트 오류율 비교



Table. 2 BERs comparison of CC and RS code at 100m range

Symbol rate (sps)	CC	RS
100		
BER	0.045	0.014
200		
BER	0.115	0.065
400		
BER	0.065	0.023

표 3. 송수신기 거리 400m에서 컨벌루션과 Reed-Solomon 코드의 비트 오류율 비교

Table. 3 BERs comparison of CC and RS code at 400m range

Symbol rate (sps)	CC	RS
100		
BER	0.014	0.062
200		
BER	0.083	0.026

400		
BER	0.039	0.012

Comparing BERs of Table 2 for 100 m and Table 3 for 400 m range, All the BERs at the same transmission conditions of former are larger than those of latter. This is due to the fact that the SNR of 100 m is less than that of 400 m range, since the fading statistics of 100 and 400 m are approximated as Rayleigh and Rice distribution, respectively.

VI. Conclusions

Error correction codes of CC and RS are adopted in very shallow water channel and their performances are evaluated based on the multipath channel characteristics. At two different source-receiver ranges of 100 and 400 m, their coherent bandwidths, multipath interference magnitudes as a function of frequency, fading statistics and temporal coherence are analyzed. The sea experiment results show that RS code has better performance than CC in frequency selective channel. In frequency non-selective channel, CC performance is better than that of RS. Both CC and RS shows better performance in Rice fading than Rayleigh fading channel.

In conclusion, RS code is found to be a better choice than CC since errors occur as bursts in very shallow water frequency selective fading channel. Since fading statistics depends on both range and frequency its effect on UWA communication system remains in future work.

ACKNOWLEDGEMENTS

This work was supported by a Research Grant of Pukyong National University. (2014Year: CD2014-0288).

REFERENCES

- [1] M. Stojanovic and J. Preisig, "Underwater acoustic communication channels: Propagation models and statistical characterization," *IEEE Communication Magazine* Vol. 47, pp. 84-89, 2009.
- [2] D. Xue, C. Seo, J. Park and J. R. Yoon, "Impact of sea surface scattering on performance of QPSK," *Journal of the Korea Institute of Information and communication engineering* Vol. 18, pp. 1818-1826, 2014.
- [3] J. Kim, K. Park, J. Park and J. R. Yoon, "Coherence bandwidth effects on underwater image transmission in multipath channel," *Japanese Journal of Applied Physics* Vol. 50, pp. 07HG05-1-07HG05-5, 2011.
- [4] K. Park, J. Park, S. W. Lee, J. W. Jung, J. Shin, and J. R. Yoon, "Performance evaluation of underwater acoustic communication in frequency selective shallow water," *The Journal of the Acoustical Society of Korea* Vol. 32, pp. 95-103, 2013.
- [5] Lv Shu and S. Xiaohong, "Research on shallow water acoustic communication based on frequency hopping," *Signal Processing, Communication and Computing (ICSPCC), 2012 IEEE International Conference on*, pp.392, 395, 2012.
- [6] N Nasri, L Andrieux, A Kachouri, and M Samet, "Efficient encoding and decoding schemes for wireless underwater communication systems," *2010 7th international multi-conference on systems, signals and Devices*, Philadelphia, pp. 1-6, 2010.
- [7] J. Park, C. Seo, K. Park and J. R. Yoon, "Effectiveness of convolution code in multipath underwater acoustic channel," *Japanese Journal of Applied Physics* Vol. 52, pp. 07HG01-1-07HG01-3, 2011.
- [8] C. Seo, J. Park, K. Park and J. R. Yoon, "Performance comparison of convolution and Reed-Solomon codes in underwater multipath fading channel," *Japanese Journal of*

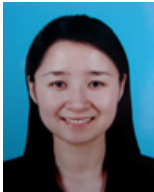
[9] John G. Proakis, and Masoud Salehi, *Digital Communications* (McGraw- Hill, New York), 5th Edition, Chap.13.

[10] T.C.Yang, "Measurements of temporal coherence of sound transmissions through shallow water," *Journa of Acousical Society of America* vol.120, no.5, Pt.1 of 2, pp.2595-2614, Nov. 2006.



배민자(Minja Bae)

1993 부경대학교 정보통신공학과 학사
1995 부경대학교 전자공학과 석사
2007~현재 : 지니테크 대표이사
※관심분야 : 수중통신, 디지털 신호 처리, 통화 품질측정 알고리즘, 패킷신호처리



설단단(Xue Dandan)

2009 중국 산시과학대학교 전자정보통신공학과 학사
2015 부경대학교 정보통신공학과 석사
2016 부경대학교 정보통신공학과 박사과정
※관심분야 : 신호 처리, 수중 음향 통신, 무선 통신



박지현(Jihyun Park)

2000 부산대학교 정보통신공학과 학사
2002 부경대학교 정보통신공학과 석사
2008 부경대학교 정보통신공학과 박사
※관심분야 : 수중 음향, 수중 통신 시스템, FPGA 설계



윤종락(Jong Rak Yoon)

1987 Florida Atlantic University Dept. of Ocean Engineering M,S
1990 Florida Atlantic University Dept. of Ocean Engineering Ph,D
1990~현재 부경대학교 정보통신공학과 교수
※관심분야 : 수중 음향, 음향 신호 처리, 음향 신호 해석 및 식별, 수중 음향 통신